The use of microscopic X-ray diffraction for the study of HgS and its degradation products corderoite (α-Hg3S2Cl3), kenhsuite (γ-Hg3S2Cl2) and calomel (Hg2Cl2) in historical paintings

Marie Radepont, Wout de Nolf, Koen Janssens, Geert van der Snickt, Yvan Coquinot, Lizet Klaassen, Marine Cotte

The use of microscopic X-ray diffraction for the study of HgS and its degradation products corderoite (α-$Hg_3S_2Cl_2$), kenhsuite (γ-$Hg_3S_2Cl_2$) and calomel (Hg_2Cl_2) in historical paintings

Marie Radepont,*[a,b] Wout de Nolf,[a] Koen Janssens,[a] Geert Van der Snickt,[a] Yvan Coquinot,[b] Lizet Klaassen[d] and Marine Cotte[b,c]

Received 15th December 2010, Accepted 7th February 2011
DOI: 10.1039/c0ja00260g

Since Antiquity, the red mercury sulfide (α-HgS), called cinnabar in its natural form or vermilion red when synthetic, was very often used in frescoes and paintings, even if it was known to suffer occasionally from degradation. The red pigment hereby acquires a black or silver-grey aspect. The chemical characterization of these alteration products is rather challenging mainly because of the micrometric size and heterogeneity of the surface layers that develop and that are responsible for the color change. Methods such as electron microscopy, synchrotron-based microscopic X-ray fluorescence, microscopic X-ray absorption near edge spectroscopy, Raman microscopy and secondary ion microscopy have been previously employed to identify the (Hg- and S-) compounds present and to study their co-localization. Next to these, also microscopic X-ray diffraction (XRD) (either by making use of laboratory X-ray sources or when used at a synchrotron facility) allows the identification of the crystal phases that are present in degraded HgS paint layers. In this paper we employ these various forms of micro-XRD to analyze degraded red paint in different paintings and to compare the results with other X-ray based methods. Whereas the elemental analyses revealed in the degradation products, among mercury and sulfur, the presence of chlorine, X-ray diffraction allowed the identification, next to α-HgS, of the Hg and S-containing compound calomel (Hg_2Cl_2) but also of the Hg, S and Cl-containing minerals corderoite (α-$Hg_3S_2Cl_2$) and kenhsuite (γ- $Hg_3S_2Cl_2$). These observations are consistent with X-ray absorption spectroscopy measurements performed at the S- and Cl-edges.

1. Introduction

The colour of painters' pigments can sometimes evolve in a manner that is unwanted or unexpected by the original artist or curator of the painting. The blackening of the red pigment vermilion is a well documented phenomenon that has been studied for a long time[1,2]. While in some papers this colour change was thought to be induced by a phase change from red α-HgS (cinnabar) to black β-HgS (metacinnabar)[1,3], recent evidence has demonstrated that other factors and chemical transformations are related to the colour change; these alteration reactions lead to the formation of different chemical species.

Different techniques were used to study the discolouration of red mercury sulfide, but each one has its assets and drawbacks. Elemental techniques such as Scanning Electron Microscopy with Energy Dispersive X-ray analysis (SEM-EDS) or X-ray fluorescence (XRF) are non-destructive, easily available and can provide a preliminary description of the samples. In particular, the presence of chlorine can be assessed, providing that the analysis is performed under vacuum. Conversely, these methods cannot provide information on the mineral composition of the degradation products. Especially, metacinnabar, corderoite (α-$Hg_3S_2Cl_2$) or calomel (Hg_2Cl_2) cannot be unambiguously identified. XRF can be performed with portable instrument directly onto the painting, while SEM-EDS will be used for a complementary microscopic analysis of painting fragments. The main advantage of synchrotron radiation (SR)-based μ-XRF towards this last technique is an higher sensitivity, which is particularly important here, as Cl can be present as a trace element.

For the molecular analyses, various methodological approaches are offered. Raman is a quite a commonly used technique for the study of paintings as it is largely available, and can be performed with portable instruments directly onto the painting. The micrometric resolution is also essential for the selective analysis of degraded superficial layers on cross-sections. In the present case, it enables the identification and

distinction of compounds such as cinnabar, metacinnabar (only if it is a major component), calomel (as done by Spring et al.[4] in a study of a degraded painting from the 15th century) or corderoite. However, as with other laser-based techniques, the primary laser flux needs to be regulated, in particular for the analysis of cinnabar which can blacken under the beam. The Raman data acquisition can also be hampered due to the presence of a high fluorescence background, especially due to the presence (in samples derived from easel paintings) of products such as organic binders and glazes.

Secondary Ion Mass Spectrometry (SIMS) is a less commonly employed technique for painting analysis but offers unique possibilities for high resolution chemical imaging. The main challenges are related to sample preparation (results are highly affected by the sample surface quality) and to data analysis. Indeed, the data interpretation can be distorted by the formation during the ion beam analysis of cluster anions, formed by recombination of different molecular groups, that are not necessarily present in the initial material. Considering this problem, analyses of pure references and their mixtures are both necessary. As an example, by analyzing a sample from a 17th painting, Keune et al.[5] have observed $(HgCl)_2.Cl^-$ clusters in the spectrum of $(HgCl)_2$ and in the one of altered sample, yet it is not possible to associate these ions in an unequivocal manner to calomel, as the $(HgCl)_2.Cl^-$ ion is also detected in the spectrum of HgS + $HgCl_2$. These results therefore are only suggestive of the presence of mercuric chloride ($HgCl_2$) in degraded HgS paint samples. Thus, even if SIMS is a valuable technique that provides molecular information on not-necessarily crystallized materials, the associated data interpretation can be delicate in the case of the materials with complex composition; this is certainly also the case when considering mercury sulfide degradation.

μ-XANES (X-ray absorption near edge spectroscopy) also offers chemical information with submicroscopic resolution and without any requirements regarding compound crystallinity. The sensitivity of this method (when XANES spectra are acquired in fluorescence mode) is also a clear advantage, particularly for the analysis of material degradation where the major elemental composition remains unchanged (Cotte et al.[6,7]). However, the currently available databases are more limited than for Raman spectrometry or X-ray Diffraction (XRD) (in particular at the Cl K-edge). It is thus sometimes difficult to clearly identify the present phases, especially in the case of complex mixtures.

It it striking to note that some methods are very sensitive and show a high specificity to distinguish between particular kinds of the molecular species (such as SIMS that allows to record maps of e.g. the soap of a particular metal such as Pb or Cu and of a specific carboxylic acid such as palmitic acid) but are insensitive to other subtle distinctions between the compounds present, that may be very valuable to understand the sequence of tranformations that leads to a visual degradation phenomenon such as the one of cinnabar.

The microscopic size of the degaradation layers, the complexity of the composition of the paint layers and the possible effect of minor and trace elements motivated Cotte et al. to start making use of synchrotron radiation based microanalytical techniques. Microscopic X-ray fluorescence (μ-XRF) and X-ray absorption near edge spectroscopy (μ-XANES) measurements were performed on samples of Pompeian wall paintings[6] in order to determine the valence state of relevant elements and obtain information on their molecular associations. This study demonstrated the presence of (light-coloured) sulfates on the surface of black degraded HgS-samples. In addition, chlorine was identified in grey altered regions of another Pompeian sample[6]. In another study on samples from Catalan altarpieces from the Gothic era, Cotte et al.[7] recorded S-K edge and Cl-K edge XANES spectra that were consistent with the presence of a mixture of HgS, calomel and α-$Hg_3S_2Cl_2$ (corderoite, a grayish-black mineral[8]) in areas where a co-localization of S, Cl and Hg was observed by μ-XRF.

Irrespective of the limitations of each separate method, these studies taken as a whole, highlight the role of chlorine or chlorine-containing compounds as reagents involved in the degradation of mercury sulfide. Yet, the exact sequence in which they are formed and therefore the role they may play during the degradation process are not fully understood, possibly because not all (intermediate) reaction products have been documented yet. In an attempt to identify in a more specific manner the (mercury) compounds present in degraded HgS paint layers, in what follows we employ different forms of X-ray diffraction (XRD) on artificially aged model samples

Methods	Portable ?	Lateral resolution	Sampling necessary ?	Specific compound identification possible ?
Lab-XRD	No	Submillimetric	No	Yes
SR µ-XRD	No	µm - tens of nm	Yes	Yes
SEM-EDS	No	Submicrometric	Yes	No
Raman microscopy	Yes	Micrometric	No	if a major component
SIMS	No	Hundred of nm	Yes	No
SR µ-XRF	No	µm - tens of nm	Yes	No
SR µ-XANES	No	Submicrometric	Yes	if a major component

Table 1: Comparison of different techniques used for the study of the degradation of mercury sulfide.

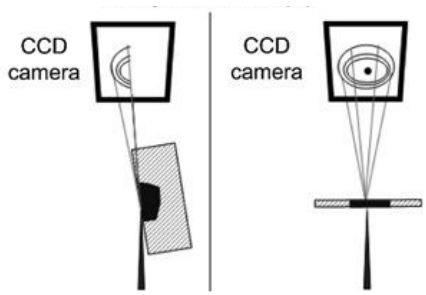

Fig 1: Reflection (left) and transmission (right) XRD geometry used resp. in the laboratory and SR-based µ-XRD instruments.

and on naturally aged original paint samples of different origin. We compare the results obtained by XRD to those obtained with other X-ray based microanalytical methods from the same samples.

2. Materials and methods

Table 1 provides an overview of the techniques already used in the past for the study of the HgS degradation and some of their characteristics. In what follows, the aged model samples and micro-samples from original works of art were analyzed by X-ray diffraction, X-ray fluorescence and X-ray absorption near edge spectroscopy.

2.1. X-ray diffraction techniques

Contrary to most of the methods mentioned in Table 1, X-ray diffraction has the unique feature that it can provide information on the crystalline phases (and their subtle changes) present in the material analysed. Two types of µ-XRD instrumentation were employed: one based on a laboratory source of X-rays and another employing synchrotron radiation. For the investigation of cultural heritage materials, the use of laboratory (µ-)XRD is quite common; however, the SR-radiation based variant is used to an increasing extent, and especially for the analysis of paintings. The microscopic size of the primary beam that can be generated at SR sources allows the characterization of each separate layer in complex stratigraphic samples. Certainly in cases where thin alteration layers, consisting of complex mixtures of different degradation products, are formed, the use of SR-based µ-XRD is very relevant, as demonstrated by Salvado et al.[9,10]. When working with XRD, in some cases it is possible to perform analyses in transmission mode, with the sample perpendicular to the incident beam (Fig. 1). In this configuration, the beam projection on the sample is smaller than in reflection mode and enables the acquisition of the complete diffraction parttern without having the sample itself blocking part of the rings (Fig. 1)[7]. Using laboratory sources, which usually employ primary energies in the 4-17 keV (Cr-K_α to Mo-K_α) range, this geometry is suitable for the study of very small fragments (of a fraction of a mm in size), or of thin sections. At SR facilities, where higher energy beams are availble (e.g., in the 25 to 100 keV range[11]), this geometry can sometimes be employed to examine entire paintings[12]. These cases excepted, direct (µ-)XRD analyses on works of art usually are carried out in reflection mode (Fig. 1)[7]. In this condition, the small angle (ca 10°) between the surface of the object and the incident beam causes the footprint of

Solution	Light	Time of ageing (hours)	Visible alteration?
NaCl (0.505 mol.L^{-1}; 3mL)	Yes	24 to 2901	Yes
NaOCl (9.60%; 3 mL)	Yes	24	No
NaOCl (9.60%; 3 mL)	Yes	48 to 741	Yes
NaOCl (9.60%; 3 mL)	No	24 to 168	No
NaOCl (9.60%; 1.5 mL) + H_20 (1.5 mL)	Yes	24 to 48	No
NaOCl (9.60%; 1 mL) + H_20 (3 mL)	Yes	24 to 48	No

Table 2: Different conditions of artificial ageing with the solutions present in the tubes, the presence of UV-visible light, the time of ageing and whether or not an alteration was visible.

the primary beam to be significantly enlarged in one direction. Also as a result of the use of lower primary energies in this scattering geometry, this type of analysis is much more surface sensitive.

a. Laboratory-based XRD

The X-ray diffraction instrument used was developed in the C2RMF laboratory[13] and is based on a Rigaku MSC MicroMax 002 X-ray tube with a copper anode (wavelength of 1.5418Å). After collimation to 200 µm, a monochromatic beam with a flux of 2x10^8 photons/s is obtained. 2D XRD patterns are collected by means of Rigaku R-axis imaging plates. FIT2D[14] is used to transform the 2D images into standard diffractograms and the software package EVA is employed to identify the crystalline phases via comparison to a database of XRD diagrams.

b. Synchrotron based µ-XRF/µ-XRD spectrometry at ESRF beamline ID18F

Synchrotron radiation allowed for the development of a diverse range of analytic tools with unique properties; among these are microanalytical methods. The combination of different microscopic techniques can provide information on the (local) elemental content, but also on the chemical state and/or on the crystalline phases that are present at specific location, and is a major asset when studying complex systems such as multi-layered paint cross-sections[9-11]. µ-XRD coupled to µ-XRF analyses were performed at beamline ID18F at the European Synchrotron Radiation Facility (ESRF, Grenoble, France)[15]. A wide energy range (6-70 keV) is obtained thanks to a Si (111) and Si (311) double crystal monochromator. The excitation energy was fixed at 28 keV and the primary beam was focussed to 5.3x1.8 µm² (hor. x ver.) by means of a compound refractive lens. Micro X-ray diffraction patterns were collected in transmission by means a CCD camera simultaneous to the recording of XRF spectra via an energy-dispersive Si(Li) detector. Details about the set-up can be found elsewhere[7,15]. XRD data were analyzed by using the XRDUA[16] software.

2.2. Combined µ-XRF and µ-XANES imaging at ESRF beamline ID21

µ-XANES coupled to µ-XRF analyses were performed at the X-ray microscope beamline ID21 of ESRF[17]. On this beamline, a highly monochromatic primary beam is obtained thanks to a fixed-exit Si(111) double crystal monochromator. The energy range is going from 2 to 9 keV with a resolution of $\Delta E/E = 10^{-4}$. At the S- and Cl-edge energies, the beam size was reduced down to 0.60x0.25 µm² (hor. x ver.) by means of Fresnel zone plates. The µ-XRF signals were collected in the horizontal plane, perpendicular to the incident beam direction, by using an energy-dispersive HPGe detector to create elemental maps and identify the different layers in the samples. Then, at a number of relevant locations, µ-XANES spectra were recorded. The resulting X-ray fluorescence spectra were fitted using the PyMCA software[18]; this was mandatory in order to differentiate the M-emission lines of mercury from the K-lines of sulfur. Batch fitting of the XRF spectra corresponding to each pixel of the 2D maps yielded elemental maps. The XANES spectra were expressed as a linear combination of a set of chlorine- and sulfur-reference compounds spectra (Excel).

2.3. Artificially aged HgS pellets

In order to reproduce the alteration seen on original works of art, artificial ageing was performed on vermilion powder samples. HgS powder (Prolabo) was finely milled and pressed into cylindrical pellets of 3 mm diameter and around 800 µm thickness that were then embedded in resin (Araldite 2020) and polished to have both faces of the pellet

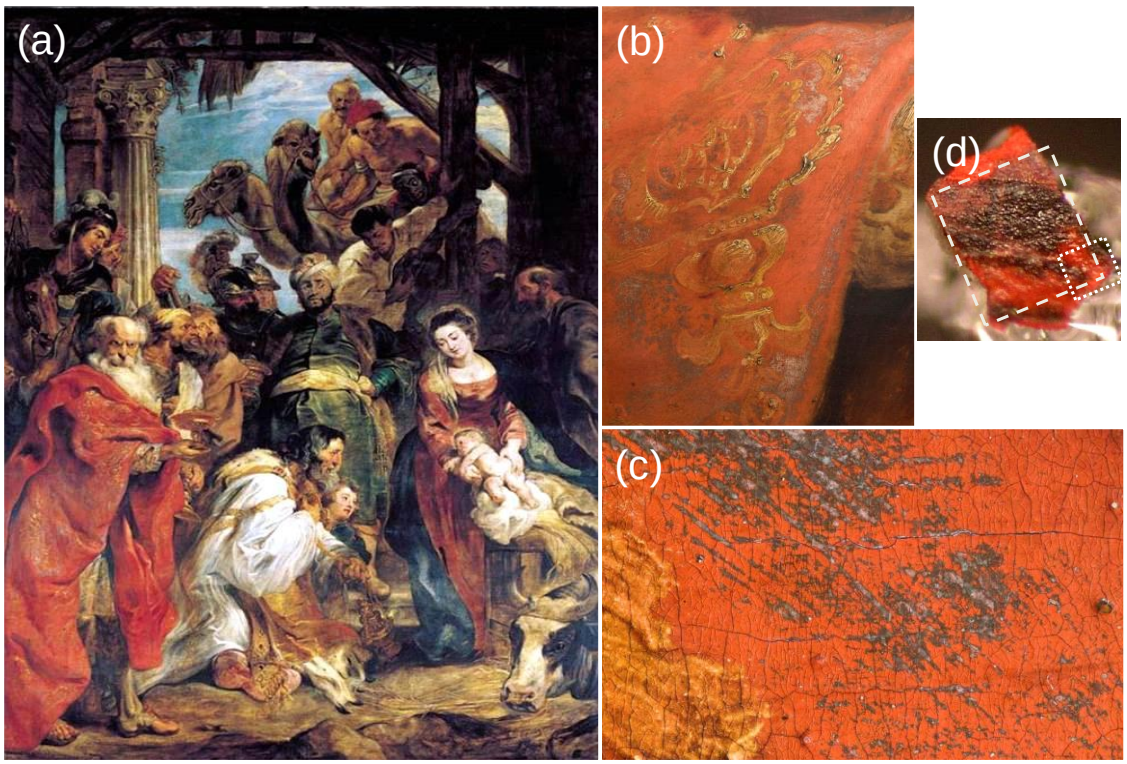

Fig 2: (a) "The Adoration of the Magi" by Peter Paul Rubens, Royal Museum of Fine Arts, Antwerp, Belgium; (b) optical photograph of a degraded area near the right sleeve of the figure on the right; (c) higher magnification photogrph showing darkened areas and white precipitates on the top surface; (d) optical micrograph of one sample analyzed. Dotted rectangle in (d) indicates scanned area of Fig. 5; dashed rectangle indicates scanned area of Fig. 6.

exposed. Prior to pressing, the HgS powder was not mixed with any binder material. The pellets were placed in tubes and exposed to various Cl-containing solutions during different periods (1 to 120 days), either under UV-Visible light irradiation or while being kept in the dark. While all the HgS pellets that were kept in the dark retained their bright red color, the ones under UV-visible irradiation in tubes containing NaOCl solution (9.6%) during more than 24 hours presented a visible alteration at the surface: a grey-violet surface featuring white cristals was formed. As shown in Table 2, the pellets exposed during equivalent periods to UV light and NaCl solution showed the beginning of an alteration but with a less evident discoloration. Material from the altered pellets was analysed using the same combination of methods as used for the characterization of 'naturally aged' HgS samples.

2.4. Original paint samples

Several small samples (smaller than 0.5 mm in all dimensions) were taken from altered areas in the monumental 17th century painting "The Adoration of the Magi" (1617-1618) by P.P. Rubens (Fig. 2). This painting is part of the collection of the Royal Museum of Fine Arts in Antwerp, Belgium. The fragments originate from the red bright cloak of the figure on the left side of the canvas; this large red area presents a discoloration in some parts; blackened areas are clearly visible. Microscopic photographs reveal that on top of the superficial black layer, white crystals have formed. A combination of µ-XRF, µ-XANES and µ-XRD was used to characterize the altered surface and cross-sections of some of these samples.

A number of paint samples taken from highly damaged paintings from the Monastery of Pedralbes, Barcelona that date to the Gothic era (14th C.) and showing a very significant blackening of the originally red HgS area, were also examined by means of µ-XRF, µ-XANES and µ-XRD under the form of thin sections (10 µm).

3. Results

3.1. Characterization of artificially aged HgS pellets

In Fig. 3, optical photographs of the artificially aged HgS

Exposure	NaCl-solution After 120 days	NaOCl-solution After 11 days	NaOCl-solution After 23 days
No irradiation (darkness)	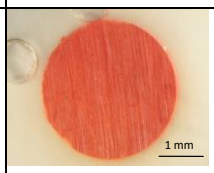	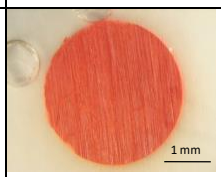	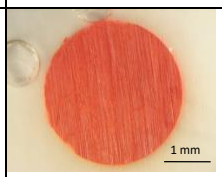
UV-visible irradiation	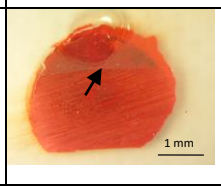	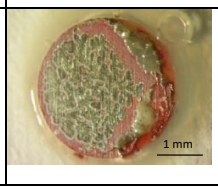	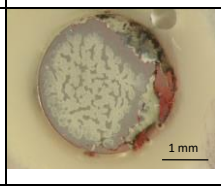

Fig 3: Optical photographs of the resin-embedded HgS pellets before (left column) and after ageing (right columns) in different circumstances. The NaCl/UV photograph was taken after 120 days of exposure whereas the NaOCl/UV photographs were taken after 11 and 23 days after exposure.

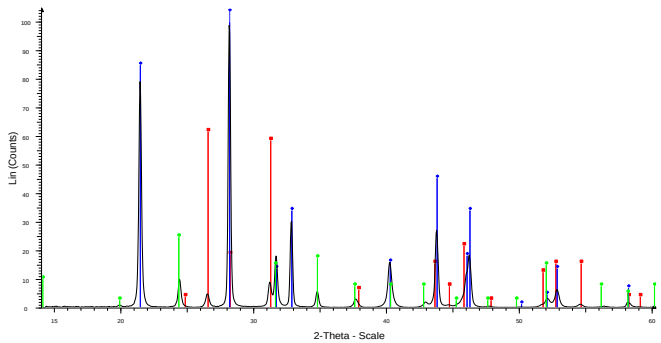

Fig 4: Diffractogram of a pellet after ageing 552 hours at room temperature in a tube containing 3mL of NaOCl (9.6%) and exposed to UV/Visible light. Red lines: cinnabar (α-HgS), blue: calomel (Hg_2Cl_2), green: corderoite (α-$Hg_3S_2Cl_2$).

pellets, during/after their exposure to NaCl and NaOCl solutions and UV-visible radiation are intercompared. Already after 24h of exposure to NaOCl, the colour of the surface gradually started to change from bright red to greenish-yellow. Clearly, the activation of the materials by UV irradiation is required to provoke the colour change. This figure also demonstrates that the alteration process is much faster in case a solution of higher oxidative power such as NaOCl rather than a NaCl solution is employed. However, provided that sufficient contact time is allowed (>120 days), the exposure to the NaCl solution under UV irradiation also leads to a (less clear) colour change of the surface.

The thickness of the pellets (0.8 mm) prevented any measurements in transmission mode with the laboratory XRD system (employing Cu-K_α radiation). Therefore, analyses were regularly performed on the pellet surfaces in reflection mode in order to identify and monitor vs. time the formation of degradation compounds. As shown in Fig. 4, next to cinnabar (α-HgS), the formation of the Cl-containing Hg compounds calomel (Hg_2Cl_2) and corderoite (α-$Hg_3S_2Cl_2$) was detected; these products were only observed in the NaOCl treated pellets that showed discolouration. For the NaCl treated pellets, the phase responsible for the slight discoloration was detectable by XRD but could not be identified. It is none of the phases identified below (see Table 3). In the pellets that retained their original colour, only the XRD peaks of α-HgS were observed.

It is noteworthy that after only one day of exposure to NaOCl, XRD examination of the discoloured pellets reveals the present of both calomel and of corderoite (α-$Hg_3S_2Cl_2$). This suggests that both products are either formed simultaneously as degradation products of HgS or that very soon after its formation, corderoite degrades further to calomel.

3.2. Original paint samples

Since in historical paint samples, and especially in those in which degradation products have formed naturally, the abundance of the (primary and secondary) materials to be identified and quantified is generally much smaller than in the model samples discussed above, the use of the laboratory based XRD instrument was not possible. Also the

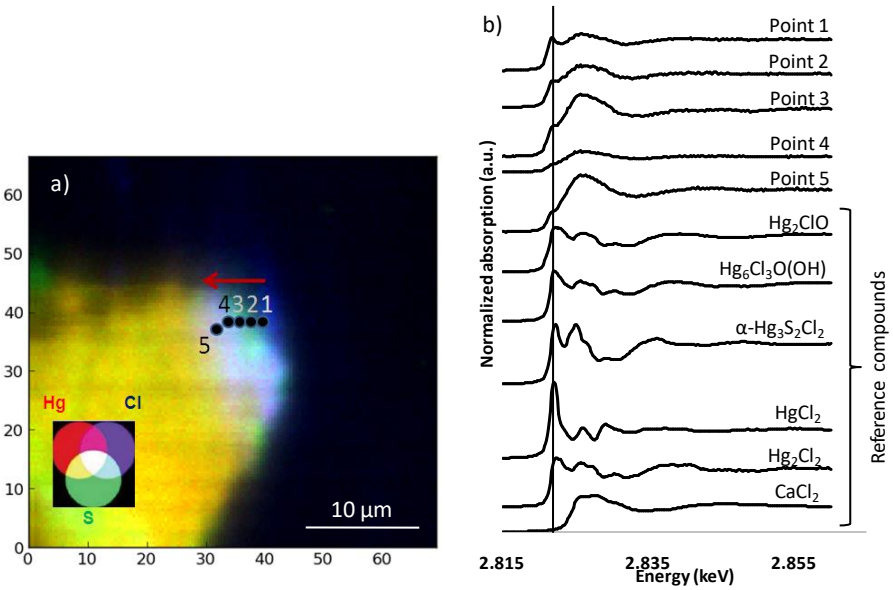

Fig 5: (a) RGB composite XRF-map of Hg, S, Cl of a corner of the sample shown in Fig. 2d. The five locations at which Cl K-edge XANES spectra were recorded are indicated; (b) Cl K-edge XANES spectra of points 1-5 and of different Hg and Cl containing reference compounds: terlinguaite (Hg_2ClO), eglestonite [$Hg_6Cl_3O(OH)$], corderoite (α-$Hg_3S_2Cl_2$), mercury chloride ($HgCl_2$), calomel (Hg_2Cl_2), and calcium chloride ($CaCl_2$). Size of map: 70x66 µm^2 (hor. x ver.).

thickness of the (alteration) layers requires the use of a primary beam that is close to 1 µm in diameter. Accordingly, SR-based µ-XRD analysis at ESRF-ID18F was combined with high-resolution µ-XRF/µ-XANES to characterize the original paint samples.

a. Characterization of historic samples from Rubens' "Adoration of the Magi"

Prior to the µ-XRD measurements, the micro sample was characterized by means of µ-XRF and by Cl K-edge and S K-edge µ-XANES at ID21, ESRF. In Fig. 5a, an RGB composite of the Hg, S and Cl maps obtained by µ-XRF scanning of a corner of the sample (dotted rectangle in Fig. 2d) is presented. On the right of the scanned area, the presence of Cl is revealed. In Fig. 5b, Cl K-edge µ-XANES spectra at the locations (marked 1 to 5 in Fig. 5a) are compared to that of a number of Cl-reference compounds. As discussed more in detail by Cotte et al.[6,7], on the basis of these data it is possible to demonstrate the presence of mercury-chloride compounds (next to other chlorides). In the XANES spectra of the former, the white line has a characteristic shape and the first inflection point of the edge is shifted towards lower energies. The exact nature of the (mixture of) Hg-Cl compounds cannot be established, since the Cl-K XANES spectra of several Hg-Cl compounds are similar. The presence of Hg-S-Cl minerals terlinguaite (Hg_2ClO) or eglestonite [$Hg_6Cl_3O(OH)$] that are characterized by very similar XANES spectra, has been suggested before[6]. Qualitative comparison of the XANES spectra in Fig. 5b also suggest that $HgCl_2$, a compound assumed by Keune et al. to be present in sample of a 17th C. painting[5] and characterized by a very sharp white line in its Cl K-edge XANES spectrum, is not (abundantly) present here; rather, the XANES spectra recorded at positions 1-3 resemble most closely those of calomel (Hg_2Cl_2) and/or terlinguaite (Hg_2ClO). Attempts to express the spectra collected at point 1-5 as a linear combination of the reference spectra shown in Fig. 5b generally failed; especially the broad feature between 2.825 and 2.830 keV is hard to describe, although the spectrum of $CaCl_2$ (and of other alkali and alkaline-earth chlorides not shown in Fig. 5b) also contain similar features. These data are therefore suggestive of the presence of a complex mixture of chlorides, some of which incorporate Hg; at the edge of the sample (position 1), the spectral feature that is specific for Hg-Cl-compounds (see vertical line in Fig. 5b) appears to be the most intense while in the area where the Hg-map (Fig. 5a) is less intense, it disappears.

In attempt to identify in a more specific manner the Hg, S and or Cl-containing compounds that are present at/near the

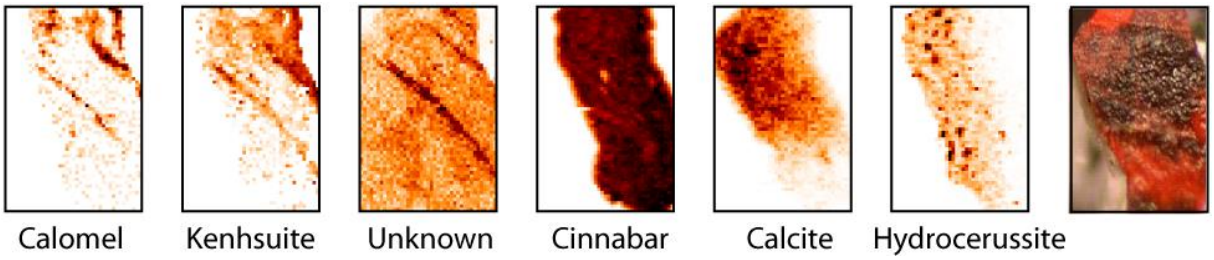

Fig 6: Diffraction maps and corresponding optical micrograph of the sample from Rubens painting, showing the projected lateral distribution of calomel (Hg_2Cl_2), kenhsuite (γ-$Hg_3S_2Cl_2$), an unknown phase (d = 7.1438 Å; d = 2.1922 Å), cinnabar (α-HgS), calcite ($CaCO_3$) and hydrocerussite [$(PbCO_3)_2.Pb(OH)_2$]. Map size: 280x300 μm^2.

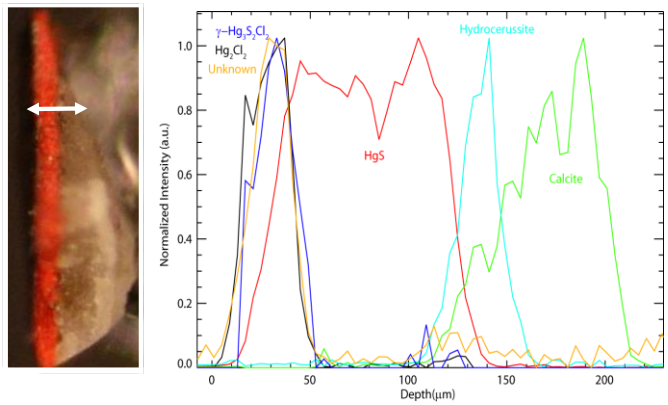

Fig 7: Depth-dependent relative abundance plot (maximum of each component normalized to unity) of several paint components in the sample shown in Fig. 2d: (left) optical micrograph indicating beam scanning path; (right) XRD intensity variation showing from right to left: the calcite ($CaCO_3$) preparation layer, the hydrocerussite [$(PbCO_3)_2.Pb(OH)_2$] ground layer, a cinnabar (α-HgS) layer and the presence of superficial calomel (Hg_2Cl_2), kenhsuite (γ-$Hg_3S_2Cl_2$) and the unidentified compound.

degraded surface, combined μ-XRF/μ-XRD mapping experiments were performed on the sample shown in Fig. 2d in transmission mode. Fig. 6 shows the distribution of calcite ($CaCO_3$, preparation layer), hydrocerussite [$2PbCO_3.Pb(OH)_2$], cinnabar (α-HgS) and of the Cl-containing compounds calomel (Hg_2Cl_2) and kenhsuite (γ-$Hg_3S_2Cl_2$) when the primary beam is moved perpendicular to the original paint surface. Also shown in Fig. 6 is the distribution of another, as yet unidentified, crystalline compound that appears to have more or less the same distribution as that of calomel and kenhsuite (d = 7.1438 Å; d = 2.1922 Å). Because the primary beam (E = 28 keV) pierces through all the paint layers of this sample, next to the components of the upper paint layers, also XRD signals from the ground layers are detected (see calcite and hydrocerussite maps in Fig. 6 and corresponding depth profiles in Fig. 7). The hydrocerussite, calcite and cinnabar maps demonstrate the grainy nature of the paint layers that are present below the superficial black layer. In the case of kenhsuite, a somewhat better co-localization with the dark colour is apparent. Kenhsuite has the same elemental composition as corderoite (α-$Hg_3S_2Cl_2$); however, while corderoite is the most stable crystalline form of $Hg_3S_2Cl_2$ and has an isometric (cubic) structure[19], kenhsuite has an orthorhombic structure[19-23] and is considered to be a metastable polymorph of corderoite. It is part of a larger series of mercury sulfohalide compounds with semi-conductor properties. The structure of both corderoite and kenhsuite can be considered to consist of a polymer of $[Hg_3S]^{2+}$ units (linked by Hg-atoms), interspersed with Cl^- ions[20]. Since kenhsuite has a canary yellow colour, at first sight it cannot be held responsible for the dark colour observed in altered HgS samples. However, both corderoite and kenhsuite are described as being sensitive to light (turning black) and decompose in alkaline conditions into HgS and HgO. Under the conditions employed for recording the maps (dwell time of only 1 s/pixel), the presence of other Hg- and Cl-containing- or of Hg, S and Cl-containing compounds such as α-corderoite could not be deduced with any certainty from the XRD data. Consistent with the Cl K-edge XANES data discussed above, no indications of the presence of crystalline $HgCl_2$ were found.

Since the black layer in Fig. 2d appears to be of a very superficial feature, this sample was also examined in another geometry, i.e. with the primary X-ray beam oriented parallel to the surface while the sample was moved sideways, progressively exposing material that is situated deeper below the surface (see Fig. 7). The resulting 'depth-profiles' of kenhsuite, calomel, the unknown phase (d = 7.1438 Å; d = 2.1922 Å), cinnabar, hydrocerussite and calcite are shown in Fig. 7. This profile show that calomel is

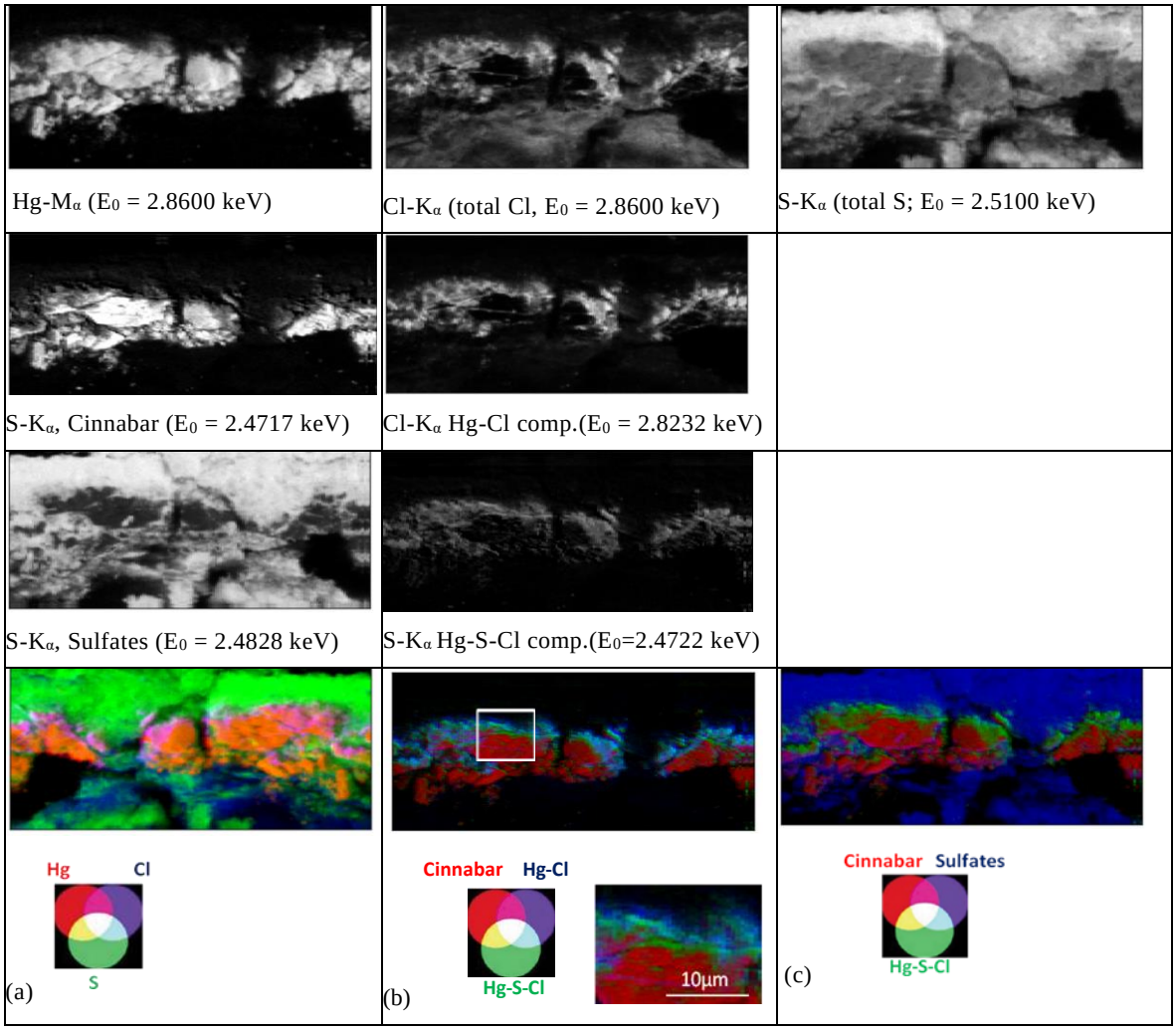

Fig 8: Element specific, Cl-species specific and S-species specific maps obtained from a cross-sectioned sample from a painting in the Predalbes Monastery, Barcelona, Spain. The presence of several layers can be discerned: layer (1) consists of of cinnabar, layer (2) of Hg-S-Cl compounds while layer (3) contains calomel. The outer layer (4) consists of sulfates (gypsum white wash layer applied in a later phase). Map size: 50×100 μm^2. Step size = 0.25×0.62μm. An enlarged portion of the Cl-species RGB composite (white rectangle) is also a shown (13×20 μm^2).

indeed exclusively present in the top layers of the sample; also the layered structure of the sample below the altered surface is clearly visible, consisting of a succession of cinnabar, hydrocerussite and calcite. In Fig. 7, the co-localization with depth of calomel, kenhsuite and the unknown compound is very clear.

b. Characterization of blackened HgS from a painting of the Monastery of Pedralbes, Spain

This above-described results encouraged us to reconsider the identification of the degradation products found in paintings from the 14th C. from the Monastery of Pedralbes, Barcelona. Samples from these strongly discoloured painting, grey and black in appearance, were previously studied by μ-XRF and μ-XANES. In order to obtain a more precise identification of these alteration products, the same samples were analysed by means of submicroscopic Cl and S K-edge XANES at ESRF-ID21 and by μ-XRF/μ-XRD at ESRF-ID18F. The results are summarized respectively in Fig. 8,9 and 10.

In the RGB composite of the elemental maps (Fig. 8a), the S-rich white wash layer (top) dominates. Below that, two layers can be discerned: the original cinnabar layer (shown orange in Fig. 8a), coated with a Hg- and Cl-containing layer (shown in magenta). Below the HgS layer, some Cl is present without Hg or S (in blue).

Over this complex stratigraphy, μ-XANES spectra were acquired at the Cl and S K-edges. In Fig. 9b, the S K-edge

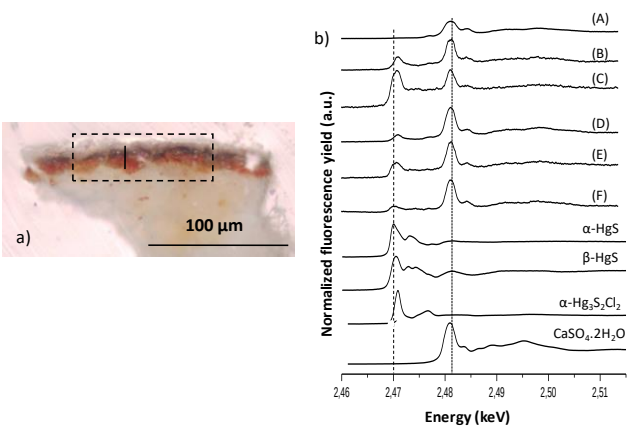

Fig 9: (a) Photograph of a thin section from the Pedralbes wall painting sample; the dashed rectangle shows the area analyzed by µ-XRF; (b) S K-edge XANES spectra of selected positions along the vertical line shown in (a) (top to the bottom), and of sulfide- and sulfate-containing reference compounds.

XANES spectra collected along the line indicated in Fig. 9a are compared to a number of sulfide and sulfate-containing reference compounds. These compounds include corderoite (α-$Hg_3S_2Cl_2$) as representative of other mercury sulfochorides; in what follow, they will be referred to as "Hg-S-Cl"-compounds. In the spectra (A)-(E), peaks are visible that coincide with the maxima of the XANES spectra of α-HgS, α-$Hg_3S_2Cl_2$ and $CaSO_4.2H_2O$. Spectrum (A) appears to indicate the presence of sulfate on the surface of the sample (top of the line) whereas in spectrum (F) (bottom of line) shows the presence of cinnabar, which is consistent with the red color of the material in the visual picture (Fig. 9a). The rest of the line is situated in a blackened layer. In this area, the corresponding spectra (B)-(E) clearly show a peak at slightly higher energy than that of α-HgS, indicative of the presence of "Hg-Cl-S" compounds.

In order to image the distribution of these various compounds in a more clear manner, XRF maps were obtained at specific energies in the vicinity of the Cl and S K-edges (Fig. 8). Two Cl-K_α intensity maps of Fig. 8b were recorded at 2.8232 and 2.8600 keV, maximizing the response of resp. the "Hg-Cl" compounds and of the totality of all chlorine species; four S-K_α maps were recorded at 2.4717, 2.4722, 2.4828 and 2.5100 keV, corresponding to the resonance energies of cinnabar, "Hg-S-Cl" compounds, sulphates and of the totality of all sulfur species (see Fig.9). The (enlarged portion of the) RGB composite of Fig. 8b

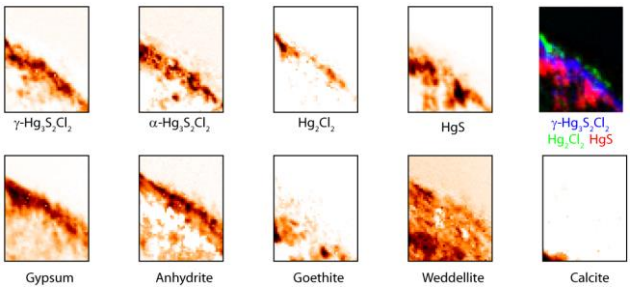

Fig 10: Diffraction maps from the Pedralbes wall painting sample, showing the lateral distribution of various mercury sulfochlorides, chlorides and sulfides (upper row), next to that of other Ca and Fe-phases. Map size: 280x300 µm^2.

suggests the presence of a 3-layered system, composed of α-HgS (layer 1), a thin intermediate layer (2) of "Hg-S-Cl" compounds with a similar XANES spectrum as corderoite (see Fig. 9) and a third layer containing "Hg-Cl" compounds. The RGB composite of Fig. 8c demonstrates that this 3-layered system is covered by a thick layer of sulfates (white wash), as is also apparent in spectrum (A) of Fig. 9b.

The diffraction maps of Fig. 10 and in particular the RGB composite of the cinnabar, kenhsuite and calomel distribution confirm the spatial ordering that was obtained by the XRF/XANES maps of Fig. 8. While the calomel is present at the outer surface of the sample (layer 3), the mercury sulfochloride compounds corderoite and kenhsuite are present in the intermediate layer (2) between calomel and cinnabar (layer 1). Although only present here in the form of a much thinner layer than in Fig. 8, anhydrite and gypsum again form a fourth cover layer on top of the calomel. Throughout all layers, crystalline weddellite (calcium oxalate) is also present, suggestive of the degradation of the binding medium.

c. Summary of observations

In Table 3, a summary of the observed Hg-compounds, as revealed by XANES spectroscopy and imaging and/or by XRD measurements is provided. In all the systems studied, chlorine proved to be involved in the degradation phenomena. A strongly oxidizing Cl-containing chemical such as NaOCl was shown to be able to attack cinnabar in a relatively short time, providing that the system is photo-activated by means of UV light. This leads to the formation of corderoite (α-$Hg_3S_2Cl_2$), itself an unstable mercury

Samples	Methods	Compounds identified			
		Hg-sulphides	Hg-sulfochlorides	Hg-chlorides	Other compounds
Artificially aged HgS pellets	Lab µ-XRD	α-HgS	α-$Hg_3S_2Cl_2$	Hg_2Cl_2	-
	SR µ-XRD	α-HgS	α-$Hg_3S_2Cl_2$	Hg_2Cl_2	-
P.P. Rubens, KMSKA, "Adoration of the Magi"	µ-XRF/µ-XANES	α-HgS	Hg-S-Cl compounds	Hg-Cl compounds	Sulfates
	SR µ-XRD	α-HgS	γ-$Hg_3S_2Cl_2$	Hg_2Cl_2	Calcite, hydrocerussite
Monastery of Pedralbes, altar piece	µ-XRF/ µ-XANES[7]	α-HgS	Hg-S-Cl compounds	Hg-Cl compounds	Sulfates
	SR µ-XRD	α-HgS	α-$Hg_3S_2Cl_2$ γ-$Hg_3S_2Cl_2$	Hg_2Cl_2	Gypsum, anhydritre, goethite, weddelite, calcite

Table 3: Summary of the results obtained by analyzing samples containing altered mercury sulfide.

sulfochloride and to (at least one) other (unidentified) degradation product.

The new aspect of our investigations of the naturally aged HgS materials is that a clear identification of two different mercury sulfochloride compounds was possible : next to corderoite, which was already assumed before[2,6], for the museum galleries throughout its entire lifetime, as well as in the wall painting from the Predalbes monastery, essentially the same compounds are encountered. In addition, neither in the Rubens or in the Predralbes samples, indications were found of the presence of crystalline $HgCl_2$, identified by Keune et al.[5] as a major degradation product.

It was previously hypothesized that corderoite originates from the degradation of cinnabar and then transforms into calomel under the influence of light[4]. The spatial ordering of the degradation layers observed by XRD mapping and the presumed instability of kenhsuite suggests that a multistep degradation process may be taking place that converts cinnabar into calomel via the following intermediates:

α-HgS → γ-$Hg_3S_2Cl_2$ → α-$Hg_3S_2Cl_2$ → Hg_2Cl_2

The particular ordering of the mercury compounds shown in Figs. 8 and 10 can be interpreted as being the result of an alteration front that slowly works itself inwards from the surface towards greater depths. As it progresses downwards, first chloride ions would be introduced into the HgS lattice (while preserving of the strong covalent bonds between Hg

first time the presence of the rare mineral kenhsuite (γ-$Hg_3S_2Cl_2$) has been identified on altered paintings. Both mercury sulfochlorides were found in layers between cinnabar and calomel and may be responsible for the black colour of the degradaded surfaces. It is also noteworthy that both in the Rubens painting, preserved in churches and en S) so that (one or more) mercury sulfochlorides are formed. In a second phase, the sulfide ions may leave this compound (possibly due to an oxidation to sulfates[5]), possibly causing a reduction of the Hg(II) to Hg(I)-ions, which finally leads to the precipitation of Hg_2Cl_2 at the surface.

However, as an alternative to the above-described linear sequence of transformations, presently, the possibility cannot be excluded that corderoite and kenhsuite are formed as two alternative degradation products from cinnabar and that both finally lose sulfur to become calomel. The precipitation of calomel at the surface of the paint samples may be caused by the fact that calomel is more soluble than both mercury sulfochlorides and therefore will more mobile within the subsurface paint during relative humidity cycles; thus, the calomel can (partially) dissolve at the depth of its formation, become transported towards the surface by moisture and, upon drying, can reprecipitate there. Moreover, the identification of both corderoite and calomel in the artificially aged pellets, even after a very short

contact time with NaOCl, may be seen as an evidence of the simultaneous transformation of cinnabar into these compounds via parallel reactions. It should be noted that all the above considerations are only hypotheses as the thermodynamic and kinetic aspects of the transformation reactions have not yet been taken into account.

From an instrumental point of view, it is clear that in order to observe the subtle differences between the mercury compounds that are present, the use microscopic XRD has been indispensable. Next to the different techniques used for the study of the degradation of mercury sulfide, X-ray diffraction is a common tool that has allowed the clear identification of non-amorphous phases, even when present as complex mixtures. Being widely used, it also benefits from the availability of large databases, which in the present case enabled us to identify (albeit with some effort) the rare mineral kenhsuite (γ-$Hg_3S_2Cl_2$) phase. As for SR-based µ-XRF, SR-based µ-XRD allowed to complement the advantages of XRD techniques with the high brightness of synchrotron sources. The use of micro beams for elemnent- and species-specific mapping by µ-XRF and/or µ-XRD is highly relevant in the present case as the size of the degradation layers is usually less than 5 µm. When available, the use of thin sections are prefered to polished cross-sections as it enables a more selective analysis of the different layers; in the latter case, the signal is integrated over the sample thickness.

4. Conclusions

In this paper, we have demonstrated the necessity of employing microscopic X-ray diffraction in combination with microscopic XRF and XANES for the study and identification of the Hg, S and Cl-containing compounds formed during alteration of cinnabar in historic paintings. The laboratory based µ-XRD system, developed at C2RMF, provides the possibility of high resolution analyses and allows for specific identification of primary and secondary crystalline phases but cannot be employed to investigate individual micrometric layers inside paint stratigraphies or other strongly heterogeneous samples. As such, its usefulness to characterize the very thin alteration layer formed during the natural degradiation of HgS in historical paintings is still limited. Another limitation is presented by the relatively low energy employed in this system, that often prevent this from being used for direct transmission analysis of paintings. SR-based µ-XRD, employing smaller and highly-energetic primary beams allow to circumvent these limitations and therefore can be used for the positive identification of components in different micrometric layers.

In the degraded historical HgS-paint samples studied here by a combination of SR-based microbeam methods, the rare mineral kenhsuite (γ-$Hg_3S_2Cl_2$) was identified for the first time. It was found to be present by itself, or as a mixture with its more stable polymorph, corderoite (α-$Hg_3S_2Cl_2$). In all cases examined, in addition also the presence of calomel (mercurichoride) was identified. Corderoite and calomel were also formed during artifical ageing of HgS pellets under UV-visible light in the presence of NaOCl solutions. However, no indications of the presence of mercurochloride ($HgCl_2$) was encountered. Likewise, contrary to the classical hypothesis, no black metacinnabar (β-HgS) was found on any of the examined altered materials. As such, only the mineral corderoite, being a mineral of purplish-grey colour has been identified as the compound that might be held responsible for the dark colour that is typical of degraded HgS-paint; all other Hg compounds identified have white or yellow aspects. On the surface of the degraded paint samples, sulfates were encountered in great abundance; part of these may have been formed during the HgS degradation, via oxidation of the sulfide ions originally present.

In order to gain more profound insights into the reaction sequence(s) that may occur during the degradation of HgS and the factors that determine their relative importance, the experiments involing artificial aging of HgS pellets and paints will be continued. Next to characterizing the mixture of Hg compounds that is present in artificially and naturally aged materials using XANES at the S and Cl-edges, also their characterization using XANES and EXAFS at the Hg-L_3 edge is likely to be relevant. Recent studies on the fate of Hg in the neighbourhood of chlor-alkali plants have shown that next to crystalline compounds such as α-HgS, corderoite and calomel, in soils, a substantial part of the Hg in the finer fraction appears to be present as amorphous Hg-S-Cl compounds; next to red cinnabar, α-HgS, also the presence of its black polymorph, β-HgS was indirectly

inferred from the Hg-L_3 edge XANES data[24,25].

Acknowledgements

The authors gratefully acknowledge GOA programme "XANES meets EELS" (University of Antwerp Research Council) and the IUAP VI/P16 programme "Nacho" (BELSPO, Brussels, Belgium) for financial support, the ESRF for granting beamtime under proposals nr. EC442 and EC720, and Gema Martinez-Criado for practical help on ID18F. Javier Chillida is thanked for providing us with the Pedralbes samples. The authors are also indebted to the Charisma programme for financial support.

Affiliations

[a] *Department of Chemistry, University of Antwerp, Universiteitsplein 1, B2610, Antwerp, Belgium. E-mail: marie.radepont@culture.gouv.fr*

[b] *Centre de Recherche et de Restauration des Musées de France – UMR171 CNRS, Palais du Louvre, 14 quai François Mitterrand 75001, Paris, France*

[c] *European Synchrotron Radiation Facility, Beamline ID21, 6 rue Jules Horowitz BP220-38043 Cedex 9, Grenoble, France*

[d] *Royal Museum of Fine Arts, Plaatsnijdersstraat 2, 2000, Antwerp, Belgium*

References

1 R. S. Davidson and C. J. Willsher, *Dalton*, 1981, 833-835.,

2 J. K. McCormack, *Min. Deposita*, 2000, **35**, 796-798.

3 R. J. Gettens and R. L. Feller, *Artists' Pigments*, 1993, 2, 167-168.

4 M. Spring and R. Grout, *National Gallery*, 2002, 50-61.

5 K. Keune and J. J. Boon, *Anal. Chem*.,2005, **77**, 4742-4750.

6 M. Cotte, J. Susini, N. Metrich, A. Moscato, C. Gratziu, A. Bertagnini and M. Pagano, *Anal. Chem.*, 2006, **78**, 7484-7492.

7 M. Cotte, J. Susini, V. A. Solé, Y. Taniguchi, J. Chillida, E. Checroun and Ph. Walter, *J. Anal. At. Spectrom.*, 2008, **23**, 820-828.

8 E. E. Foord and P. Berendsen, *The American Min.*, 1974, **59**, 652-655.

9 N. Salvado, S. Buti, J. Nicholson, H. Emerich, A. Labrador and T. Pradell, *Talanta*, 2009, **79**, 419-428.

10 N. Salvado, S. Buti, A. Labrador, G. Cinque, H. Emerich and T. Pradell, Anal. Bioanal. Chem., 2010,

11 G. Van der Snickt, J. Dik, M. Cotte, K. Janssens, J. Jaroszewicz, W. De Nolf, J. Groenewegen and L. Van der Loeff, *Anal. Chem.*, 2009, **81**, 2600-2610.

12 J. Dik, oral communication, *SR2A*, 2010, Amsterdam.

13 A. Duran, J. Castaing and Ph Walter, *Appl. Phys. A*, 2010, **99**, 333-340.

14 www.esrf.eu/computing/scientific/FIT2D

15 A. Somogyi, M. Drakopoulos, L. Vincze, B. Vekemans, C. Camerani, K. Janssens, A. Snigirev and F. Adams, *X-Ray Spectrom.*, 2001, **30**, 242-252.

16 http://xrdua.ua.ac.be

17 J. Susini, M. Salome, B. Fayard, R. Ortega and B. Kaulich, *Surf. Rev. Lett.*, 2002, **9**, 203-211.

18 V. A. Sole, E. Papillon, M. Cotte, Ph. Walter, J. Susini, *Spectrochim Acta - Part B Atom. Spectros.*, 2007, **62**, 63-68.

19 J. K. McCormack and F. W. Dickson, *The Canadian Min.*, 1998, **36**, 201-206.

20 S. Durovic, *Acta Crytallographica Section B – Structural Crystallography and Crystal Chemistry*, 1968, **24**, 1661-1664.

21 H. L. Chen, H. M. Kuang, W. T. Chen, S. M. Ying, J. H. Liu, *J. Chem. Res.-S*, 2009, **7**, 430-432.

22 N. V. Pervukhina, V. I., Vasil'ev, S. A. Magarill, S. V. Borisov, D. Yu. Naumov, *The Canadian Min*, 2006, **44**, 1239-1246.

23 S. V. Borisov, S. A. Magarill, N. V. Pervukhina, *J. Struct. Chem.*, 2009, **50**, 853-860.

24 A. Santoro, R. Terzano, G. Blo, S. Fiore, S. Mangold, P. Ruggiero, *J. Synchr. Rad.*, 2010, **17,** 187-192.

25 R. Terzano, A. Santoro, M. Spagnuolo, B. Vekemans, L. Medici, K. Janssens J. Gottlicher, M. A. Denecke, S. Mangold, P. Ruggiero, *Env. Pollution*, 2010, **158,** 2702-2709.